Thermal performance comparison of vertical and diagonal flow configurations in corrugated plate heat exchanger

Frontiers in Engineering and Built Environment

Salman Al-Zahrani
Department of Mechanical Engineering, Al-Baha University, Al Baha, Saudi Arabia

Received 12 February 2024
Revised 26 April 2024
Accepted 29 May 2024

Abstract

Purpose – The purpose of this study is to compare the thermal performance of two flow configurations in corrugated plate heat exchanger (CPHE): vertical flow configuration ($CPHE_{vert.}$) and diagonal flow configuration ($CPHE_{diag.}$). The study aims to determine the differences between these configurations and evaluate their respective thermal performance based on metrics such as heat transfer rates, pressure drop values and flow distribution.

Design/methodology/approach – The study compares the thermal performance of two flow arrangements of CPHE using identical geometrical dimensions and test conditions. Computational fluid dynamics (CFD) is employed, and a validated numerical model is used for the investigation. The comparison is based on analyzing the rate of heat transfer and pressure drop data between the two flow arrangements.

Findings – The findings indicate that the diagonal flow configuration in CPHEs offers improved flow distribution, enhanced heat transfer performance and lower pressure drop compared to the vertical flow configuration. However, the differences in general in the thermal performance of $CPHE_{vert.}$ and $CPHE_{diag.}$ are found to be minimal.

Originality/value – To the best of the author's knowledge, this study represents the first attempt to investigate the impact of vertical and diagonal flow configurations on the thermal performance of the CPHE.

Keywords Plate heat exchanger, Vertical flow, Diagonal flow, Heat transfer, Pressure drop, Thermal performance

Paper type Research paper

Nomenclature

A	Effective heat transfer area, m^2
$A_\circ$	Cross-sectional channel flow heat transfer area, m^2
C_p	Specific heat, $J/kg.k$
d_e	Equivalent diameter
f	Fanning friction factor
j	Colburn factor
JF	JF factor
h	Convective heat transfer coefficient, W/m^2K
L_h	Horizontal length from port to port, m
L_p	Plate's channel effective length, m

The author would like to thank the advanced computing Unit, King Abdulaziz City for Science and Technology (KACST), Riyadh, Saudi Arabia.

Conflict of interest: The author states that there is no conflict of interest.

Frontiers in Engineering and Built Environment
Vol. 4 No. 4, 2024
pp. 233-252
Emerald Publishing Limited
e-ISSN: 2634-2502
p-ISSN: 2634-2499
DOI 10.1108/FEBE-02-2024-0004

L_v	Vertical length from port to port, m	Subscripts	
		avg	Average
L_w	Flow channel width, m	b	Bulk fluid temperature
N	Number of channels	c	Cold stream
Nu	Nusselt number	CPHE	Corrugated plate heat exchanger
Q	Heat transfer rate, W		
Re	Reynolds number	FPHE	Flat plate heat exchanger
t	Plate thickness, m	HE	Heat exchanger
		h	Hot stream
Greek		i	Inlet condition
β	Chevron angle, °	PP	Pumping power
μ	Dynamic viscosity, $Pa.s$	o	Outlet condition
μ_t	Turbulent viscosity , $Pa.s$	w	Wall
ρ	Fluid density, kg/m^3		

1. Introduction

The escalating global energy demand serves as a catalyst for the development of a new generation of compact heat exchangers (HEs). Over the next two decades, energy demand is projected to rise by 37% (World Energy Outlook, n.d.). The corrugated plate heat exchanger (CPHE) is the most prevalent type of compact HEs. CPHE was initially introduced in the 1920s for milk pasteurization, and it was constructed as cast metal plates stacked within a frame. However, their application in more aggressive environments, such as acid coolers, was limited due to temperature and pressure constraints. Nonetheless, advancements in materials technology have enabled CPHEs to be utilized in high-pressure and high-temperature applications (Syed, 1992).

Despite its remarkable thermal performance, the immediate adoption of CPHE technology by air conditioning and refrigeration companies was hindered by the use of gaskets for sealing (Ayub, 2003). However, the introduction of welded plate HEs eliminated the need for gaskets. Presently, welded CPHEs find applications in heating, ventilation and air conditioning (HVAC) systems and ammonia cooling units (Ayub, 2003; Ham *et al.*, 2023; Mikhaeil *et al.*, 2023). In addition to their high thermal efficiency, CPHEs offer a reduced weight and volume, approximately 20 and 30%, respectively, compared to shell and tube HEs of equivalent heat transfer area (Sundén and Manglik, 2007). Furthermore, for equivalent thermal performance, the volume of CPHEs is, respectively, 50 and 60% less than that of finned tube and serpentine HEs (Li *et al.*, 2011). Consequently, CPHEs have gained widespread adoption in various industries including chemical processing, pharmaceuticals, polymers and industrial sectors. Overall, the importance of CPHEs lies in their ability to deliver enhanced heat transfer efficiency, compactness, scalability, adaptability, improved thermal performance, reliability and durability. These qualities make CPHEs a preferred choice for a wide range of industrial and commercial applications, contributing to improved energy efficiency and sustainable thermal systems.

The angle between the vertical and horizontal axes on the surface of the thermal plate of CPHE is known as the chevron angle (β). The effect of β i.e. 30°/30°, 60°/60° and 30°/60° on the thermal performance of CPHE has been undertaken by Khan *et al.* (2010). It has been found that the highest β yields both the highest Nusselt number (Nu) and friction factor (f) followed by the mixed plates, i.e. 30°/60°. Similar studies that are conducted to reveal the impact of β have reported consistent findings that Nu and f increase as β increases (Elias *et al.*, 2014; Kan *et al.*, 2015; Kwon *et al.*, 2009; Saha and Khan, 2020; Kumar *et al.*, 2018; Kılıç and İpek, 2017). Moreover, Zhang *et al.* (2019) have carried out a comprehensive review for the studies of CPHE and highlighted that β has the most significant influence on the performance of CPHE. The impact of air bubble injection on the fluid flow inside the channels of CPHE has been carried out by Marouf *et al.* (2022). Their findings revealed an increase of up to 12.4 and 14.6% in the number of transfer units (NTU) and effectiveness, respectively.

The industrial sector has witnessed continuous development, leading to numerous research efforts aimed at improving the performance of CPHE. Göltaş *et al.* (2022) have introduced plate heat exchanger (PHE) with lung-pattern surface and better thermal performance with respect to the conventional CPHE is reported. Moreover, a new shape channel named as airfoil corrugation has been proposed by Nguyen *et al.* (2022). The findings show 17% reduction in pressure drop while maintaining the same heat transfer rate as conventional CPHE. Also, a newly wavy surface of PHE is proposed by Vitillo *et al.* (2015). A new surface modification in CPHE is proposed by Al-Zahrani *et al.* (2020a) – up to 3 times enhancement in the convective heat transfer and 1.7 times increase in f data with respect to the conventional CPHE are reported. The performance of PHE with three shapes of plate surface, namely flat, asterisk pattern and corrugated pattern, have been experimentally examined by Durmuş *et al.* (2009). The corrugated pattern is found to provide both the highest Nu and pressure drop data. Likewise, the impact of the channel height of CPHE has been investigated by Islamoglu and Parmaksizoglu (2003). It has been found that Nu and pressure drop increase as the channel's height increases. A new flow arrangement for flat and corrugated PHE has been proposed by Al-Zahrani *et al.* (2021a, b), and enhanced convective heat transfer is reported. The influence of incorporating wire inserts with different diameters in CPHE channels was examined by Panday and Singh (2022). The study revealed that the increase in pressure drop outweighs the improvement in heat transfer.

Recently, researchers have increasingly adopted a multi-objective approach to optimize the design of CPHEs. By employing mathematical optimization algorithms, these methods explore the trade-offs between conflicting objectives, promoting innovation and flexibility in HE design. This approach provides engineers with a deeper understanding of the design space and the inherent trade-offs that need to be considered. Yicong *et al.* (2023) carried out a numerical study to optimize the structural parameters of the CPHE. The maximum JF has been reported to take place at $\beta = 45.49°$, corrugation pitch (P_c) of 15.13 mm and corrugation height (b) of 3.005 mm. Additionally, Shokouhmand and Hasanpour (2020) conducted a numerical study to find the trade-off between the pressure drop and the effectiveness of the CPHE's hot side. The values of the design parameters have been reported. Lee and Lee (2013) have numerically carried out shape optimization for PHE with dimples and protrusions by adopting a multi-objective optimization method/algorithm. It has been found that the ratio of dimple depth to dimple diameter has a significant influence on f data. An experimental study has been carried out by Chen *et al.* (2022) to optimize the performance of the CPHE. The effectiveness and the pressure drop are considered objective functions. The flow rate ratio has been reported to have the most significant influence on the effectiveness of the CPHE. Numerous research groups have conducted similar studies, employing a multi-objective approaches to optimize the design and performance of the CPHE (Meng *et al.*, 2023; Nguyen *et al.*, 2024; Tavallaei *et al.*, 2023; Wang *et al.*, 2023; Yu *et al.*, 2024; Alfwzan *et al.*, 2023). The performance of gas-gas CPHE employed in cabinet cooling systems, with cross- and counter-flow arrangements has been studied by Borjigin *et al.* (2020). They reported that cross-flow CPHE yields greater cooling rates compared to counter-flow CPHE. However, it is worth mentioning that the dimensions of the cross-flow CPHE are greater than those of the counter one. The performance of three types of PHEs employed in waste heat recovery from stenter machines, namely flat-PHE, wavy-PHE and zigzag-PHE, has been investigated by Jin *et al.* (2024). The findings revealed that the wavy-PHE exhibited enhanced heat transfer efficiency, primarily attributed to the significant generation of secondary flow. The crystallization of calcium carbonate in CPHE has been experimentally investigated by Berce *et al.* (2023). Infrared thermography observations along with flow and temperature measurements are utilized to monitor the fouling inside the CPHE's channels. They reported that the presence of fouling significantly distorts the isotherms, resulting in a complete skewness when compared to the clean state. This skewing effect serves as a distinct signal of channel blockage and flow obstructions, subsequently leading to substantial flow redistribution across the entire channel.

The current investigation introduces a thermal performance comparison between the vertical and diagonal flow configurations inside CPHE. The numerical tests are conducted for single-phase (cold water-hot water) and for counter-current flow arrangements at Re ranging from 500 to 3,000. Furthermore, numerous numerical studies omit the port effect, i.e. (Zhu and Haglind, 2020; Lee and Lee, 2014, 2015); however, it is considered in the present study. Additionally, the hot side is considered the process fluid in the current investigation, and thus, all calculations are performed with respect to the hot side.

2. Illustration of the present flow configuration

In CPHEs, the flow configuration can be categorized as vertical and diagonal flow configurations. In the vertical flow configuration, the fluid enters the HE from one port, i.e. the top side and flows vertically downwards between the plates to exit from the port that is located on the same side as exhibited in Figure 1a. On the other hand, in diagonal flow, the fluid enters the HE from one corner and flows diagonally across the plates before exiting through the opposite corner, as illustrated in Figure 1b.

The Chevron-type CPHE comprises several distinct geometric characteristics, as depicted in Figure 2. The dimensions associated with these characteristics of the present CPHEs are presented in Table 1.

3. Numerical models setup

3.1 Models and grids creation

The two models of CPHEs are created using Solidworks software. Each model consists of five thermal plates, with four channels distributed equally between the hot and cold channels. Careful attention is given to avoid any geometry flaws that may affect the simulation accuracy, i.e. slivers, and misalignments between plates. By meticulously constructing the models, these geometry flaws are eliminated, ensuring reliable and accurate simulation results. The models are identical except for the flow configuration, with one representing vertical flow and the other representing diagonal flow.

To capture the flow behavior and heat transfer phenomena, the grids are generated using Ansys software 19.2. When generating the mesh, several important aspects should be considered. Primarily, the mesh should have sufficient resolution to accurately represent the flow features and temperature gradients. Furthermore, the mesh should be properly structured to minimize numerical errors and provide reliable results. In the scope of this investigation, the CPHEs are made of intricate geometries characterized by irregular shapes and intricate surface features. To accurately capture these complexities, an unstructured mesh consisting of tetrahedral elements was employed, as exhibited in Figure 3.

This meshing approach grants precise control over the placement of mesh elements, facilitating their strategic arrangement to conform to the curved surfaces, irregular boundaries and intricate details of the CPHE. Consequently, a more precise and realistic representation of the flow and heat transfer behavior within the CPHE is achieved. Moreover, the adoption of an unstructured mesh offers notable advantages in terms of resolution within regions of particular interest. Certain areas within the CPHE, such as plate surfaces, corners

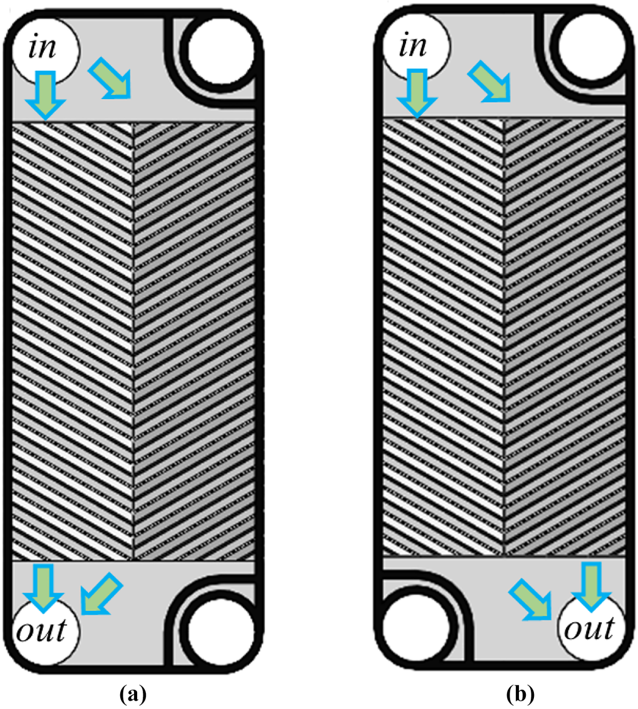

Source(s): Figure by author

Figure 1. Thermal plate of CPHE illustrates (a) vertical flow configuration and (b) diagonal flow configuration

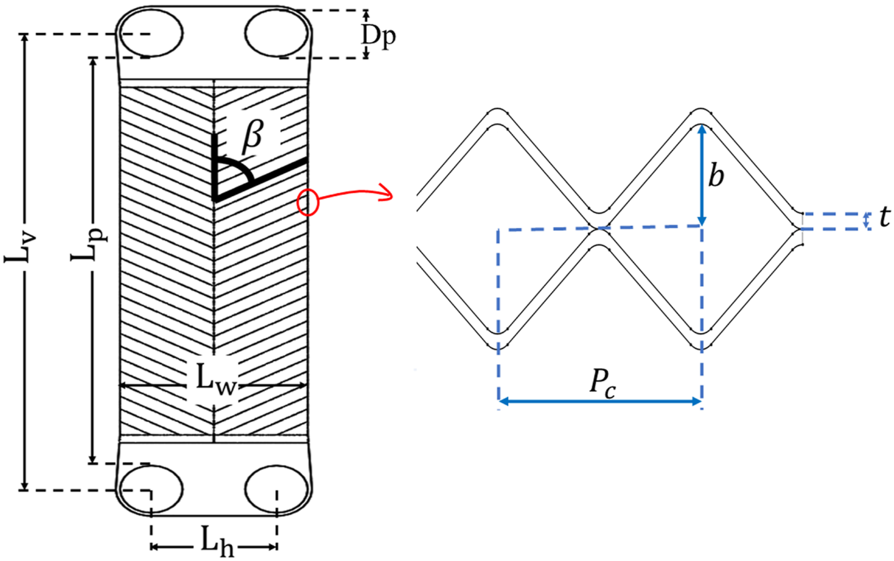

Source(s): Figure by author

Figure 2. Geometric characteristics associated with the chevron plate configuration

and regions characterized by high velocity gradients, play a pivotal role in capturing crucial flow and heat transfer phenomena. By utilizing an unstructured mesh of tetrahedral elements, this study ensures the flexibility necessary to accurately represent the intricate geometries associated with CPHEs and facilitates local mesh refinement within these regions of interest. This refined mesh allocation enables improved accuracy and computational efficiency by carefully concentrating computational resources where they are most needed (ANSYS, n.d.). Consequently, the overall computational cost of the simulation is reduced while maintaining a high level of precision and reliability. Moreover, the mesh metrics must satisfy the minimum requirements of acceptable mesh standards (ANSYS, 2009), which is fulfilled in this study. In this investigation, the grid generation process involves adjusting the sizes of the elements, starting from 0.001 m and gradually refining them to 0.0002 m, until stable grids are achieved. The goal was to create grids with sufficient resolution while maintaining computational efficiency. After several iterations, stable grids were obtained for each CPHE model, with each grid containing approximately 20 million elements. The careful selection of grid size and refinement ensured that the simulations captured the intricate flow patterns and heat transfer characteristics within the CPHEs. To assess the sensitivity of the grid, a grid sensitivity test is conducted. The results of this test are depicted in Figure 4, which showcases the variations in the local velocity as the grid is refined.

Table 1. Dimensions of the geometric characteristics of the present study

Vertical distance comprising the ports, L_v (*mm*)	560
Horizontal distance comprising the ports, L_w (*mm*)	166
Port diameter, dp (*mm*)	60
Horizontal spacing between the centers of the ports, L_h (*mm*)	106
Plate thickness, *t (mm)*	0.5
Corrugation depth, *b (mm)*	2.1
Corrugation pitch, P_c *(mm)*	10
Chevron angleβ	60°/60°

Source(s): Table by author

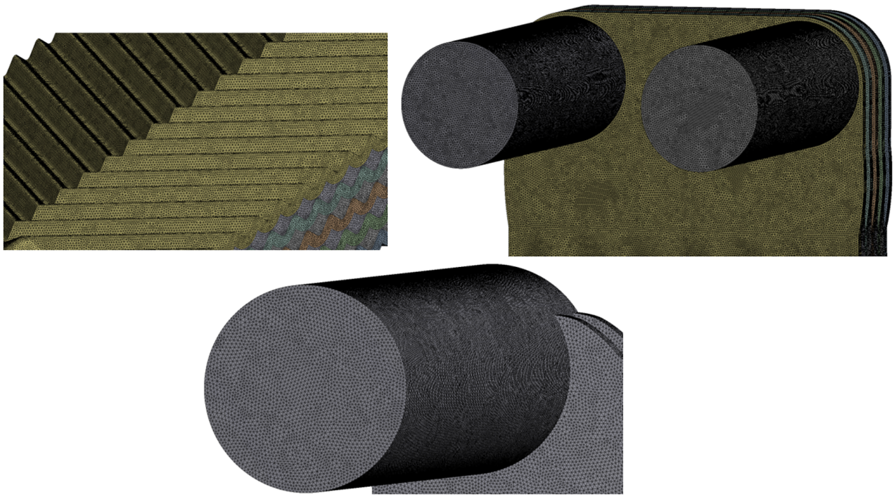

Figure 3. Zoomed views highlighting the mesh configuration employed in multiple areas of the CPHE

Source(s): Figure by author

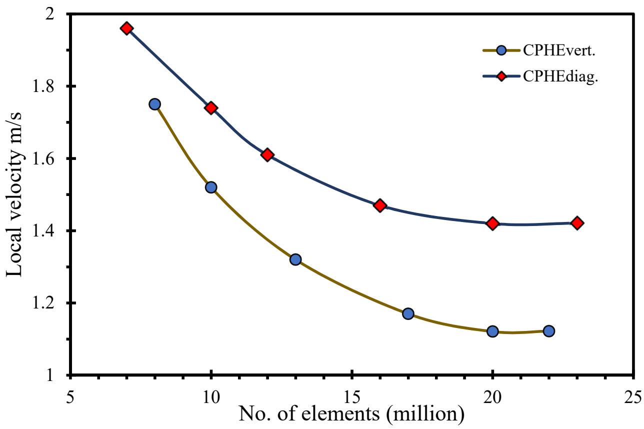

Source(s): Figure by author

Figure 4.
Mesh sensitivity tests of $CPHE_{vert.}$ and $CPHE_{diag.}$

3.2 Assumptions and governing equations

In the present study, the numerical investigation is performed on single-phase water-water as the working fluids. The analysis incorporates the following assumptions:

(1) The physical properties of both the working fluids and the material of the plates are assumed to be constant.

(2) The flow is considered to be steady, implying that there are no temporal variations in the flow characteristics.

(3) The working fluids are treated as incompressible, neglecting any changes in fluid density due to pressure or temperature fluctuations.

(4) Turbulent flow conditions are assumed, as it is widely recognized that CPHEs exhibit turbulent flow even at low Reynolds numbers i.e. Re > 400 (Gherasim *et al.*, 2011).

To effectively model flow and heat transfer phenomena in HEs, it is essential to solve the Navier–Stokes, conservation of mass and energy equations. By solving Navier–Stokes Eq.(1), momentum conservation is captured, facilitating the determination of velocity and pressure fields.

$$\frac{\partial}{\partial x_j}(\rho u_i u_j) = -\frac{\partial p}{\partial x_i} + \frac{\partial}{\partial x_j} + \left[(\mu + \mu_t)\frac{\partial u_i}{\partial x_j}\right] \tag{1}$$

The conservation of mass Eq. (2) guarantees mass conservation by equating mass rates within the system.

$$\frac{\partial}{\partial x_i}(\rho u_i) = 0 \tag{2}$$

Furthermore, the energy Eq. (3) accounts for energy conservation, enabling the prediction of temperature distribution and heat transfer rates.

$$\rho C_p \frac{\partial}{\partial x_j}(u_j T) = k_{eff} \frac{\partial^2 T}{\partial x_j^2} + (T_{ij})_{eff} \frac{\partial u_i}{\partial x_j} \tag{3}$$

3.3 Boundary conditions and model validation

The utilization of full CAD models entails a large grid element count, demanding substantial computational resources. Nonetheless, to ensure precision and closer representation of real-world scenarios, the complete CPHEs have been incorporated. Figure 5 illustrates the computational domain and boundary conditions employed in the current models, wherein mass flow rate is specified at the inlets and zero-gauge pressure is maintained at the outlets.

Computational fluid dynamics (CFD) offers a wide range of numerical models that provide designers with the flexibility to choose the most appropriate model for achieving accurate results. In the context of industrial applications, the $k-\varepsilon$ and SST $k-\omega$ models have emerged as the most widely utilized numerical models (ANSYS, n.d.). When dealing with HEs, such as CPHEs, it is crucial to carefully assess the performance of different numerical models. The accuracy of all numerical models has been scrutinized in previous studies (Al-Zahrani *et al.*, 2019, 2020b, 2021c). Among the evaluated models, the realizable $k-\varepsilon$ model has demonstrated the highest level of accuracy when compared to benchmark experimental data from the literature. The deviations between the numerical and experimental measurements for heat transfer and pressure drop are found to range from +13% to +1.3% (Al-Zahrani *et al.*, 2019, 2020b, 2021c).

4. Data reduction

The calculations presented in this study pertain to steady-state flow within a single-phase system. The hydraulic diameter (d_e) is determined as follows:

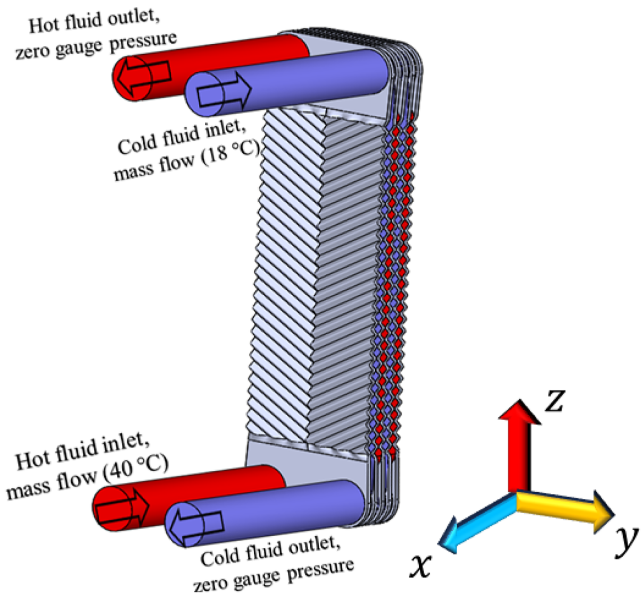

Source(s): Figure by author

Figure 5.
A schematic representation of the computational domain and associated boundary conditions

$$d_e = 2b \tag{4}$$

The parameter b represents the corrugation depth, and Re is carried out using the following approach:

$$Re = \frac{\dot{m}\, d_e}{\mu\, A_\circ N} \tag{5}$$

The crucial measurements in this analysis are the outlet temperatures of the cold and hot fluids as well as the temperature of the hot wall. The initial conditions have been set for the inlet temperatures and inlet mass flow rate. To assess the enhancement in heat transfer, the Nusselt number (Nu) is utilized. In this context, the product fluid is regarded as the hot side of the CPHE, while the utility fluid represents the cold side. Consequently, the Nu data are specifically considered for the hot side of this study. The Nusselt number (Nu) is determined by the following equation:

$$Nu = \frac{h_h d_e}{k} \tag{6}$$

The determination of the heat transfer coefficient (h_h) is performed as follows:

$$Q_h = \dot{m}_h c_{p,h} (T_{h,i} - T_{h,o}) \tag{7}$$

The data of the specific heat capacity ($c_{p,h}$) are obtained from the thermodynamics tables at the hot fluid's bulk mean temperature.

$$T_{h,b} = \frac{(T_{h,i} + T_{h,o})}{2} \tag{8}$$

It should be noted that the calculation of Q_c is derived from the equation presented as Eq. (9). Similarly, $c_{p,c}$ is determined by extracting data at the bulk mean temperature of the cold fluid, as demonstrated in Eq. (10). Energy balance dictates that the difference between Q_h and Q_c should always be zero. However, in approximately 94% of the present simulations, the difference is within the range of ±3%, while for the remaining simulations, it varies between ±5–7%. Consequently, Q_{avg}, which represents the average value of the hot and cold heat loads, is adopted for the current calculations.

$$Q_c = \dot{m}_c c_{p,c} (T_{c,o} - T_{c,i}) \tag{9}$$

$$T_{c,b} = \frac{(T_{c,i} + T_{c,o})}{2} \tag{10}$$

With the determination of Q_{avg}, the heat transfer coefficient h_h can now be calculated as follows:

$$h_h = \frac{Q_{avg}}{A(T_{h,b} - T_{w,h})} \tag{11}$$

Now, fanning friction factor (f) is estimated as follows:

$$f = \frac{\rho d_e \Delta P}{2 L_P G^2} \tag{12}$$

Where L_P denotes the effective vertical length of the plate and G represents the mass flux. Furthermore, the estimation of G is obtained through the following equation:

$$G = \frac{m^{\cdot}}{L_w b N} \tag{13}$$

5. Results and discussion

The present study involves two CPHEs with distinct flow arrangements: CPHE with a vertical flow configuration ($CPHE_{vert.}$) and CPHE with a diagonal flow configuration ($CPHE_{diag.}$). Both HEs feature identical geometrical dimensions and physical test conditions. A comprehensive comparison of thermal performance is carried out between these two HEs. Each CPHE consists of four channels, distributed alternately and equally between the cold and hot sides. Numerical tests are carried out on a single-phase (water-water), with data computed for the hot side of each CPHE over Re range spanning from 500 to 3,000. To the best of the author's knowledge, this study represents the first attempt to investigate the impact of vertical and diagonal flow configurations on the thermal performance of the CPHE. It is worth noting that Cooper and Usher (1983) have previously suggested superior thermal performance in diagonal port configurations, although their claim has not been substantiated by any previous study.

5.1 Fluid flow topology

Fluid flow inside a CPHE is a complex phenomenon that plays a crucial role in the efficient transfer of heat between two fluids. The presence of corrugated plates creates a turbulent flow pattern, facilitating enhanced heat exchange. As the fluids pass through the narrow channels formed by the plates, they experience increased turbulence and velocity due to the corrugation. This turbulent flow helps to minimize boundary layer formation and promotes efficient heat transfer between the fluids. Additionally, the compact nature of the CPHE allows for a significant reduction in size and weight compared to traditional HEs, making them ideal for various industrial applications where space is limited. The fluid flow inside the same channel of the present vertical and diagonal CPHEs has been scrutinized. The velocity contours inside this channel of $CPHE_{vert.}$ and $CPHE_{diag.}$ are illustrated in Figure 6a and b, respectively. It shows that the flow velocity within the vertical arrangement exhibits a slight superiority compared to its diagonal counterpart. Nevertheless, both contours' plots illustrate a similar flow behavior.

To provide a better understanding and visualization of the fluid flow patterns within the present CPHEs, velocity vectors inside the same channel are exhibited in Figure 7. It can be seen that both channels yield a similar flow pattern of high and low velocity vectors. For a more comprehensive graphical representation of fluid flow velocities within these channels, Figure 8 showcases the magnified area displayed in Figure 7, enabling a detailed examination.

Both representations of the velocity vectors in Figure 8a and b show a tendency to flow sideways away from the middle of the channel. This can be attributed to the fact that CPHEs are composed of angled-corrugated thermal plates, which introduce centrifugal forces exerting an outward radial force on the fluid, leading to its movement toward the sides of the channel. Furthermore, these findings align with the experimental visualization conducted by

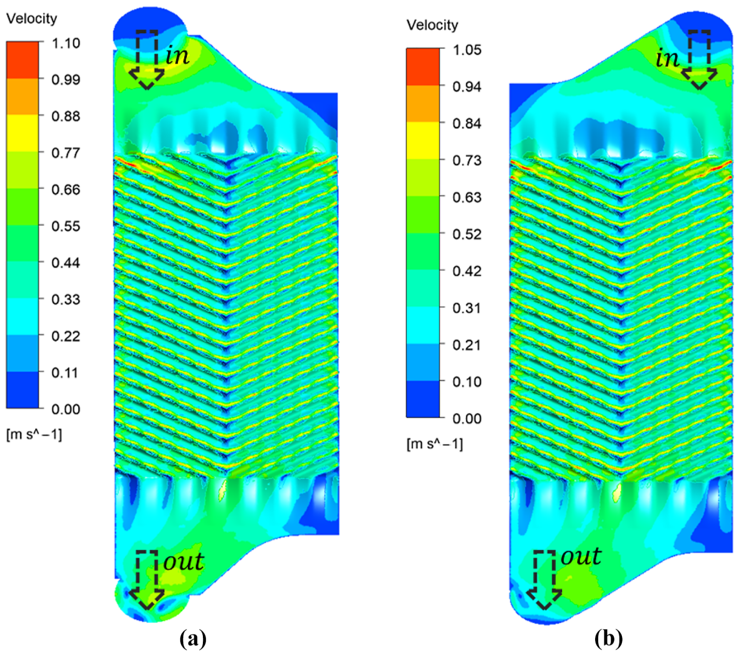

Source(s): Figure by author

Figure 6.
Velocity contours inside the hot channel for (a) vertical flow configuration and (b) diagonal flow configuration

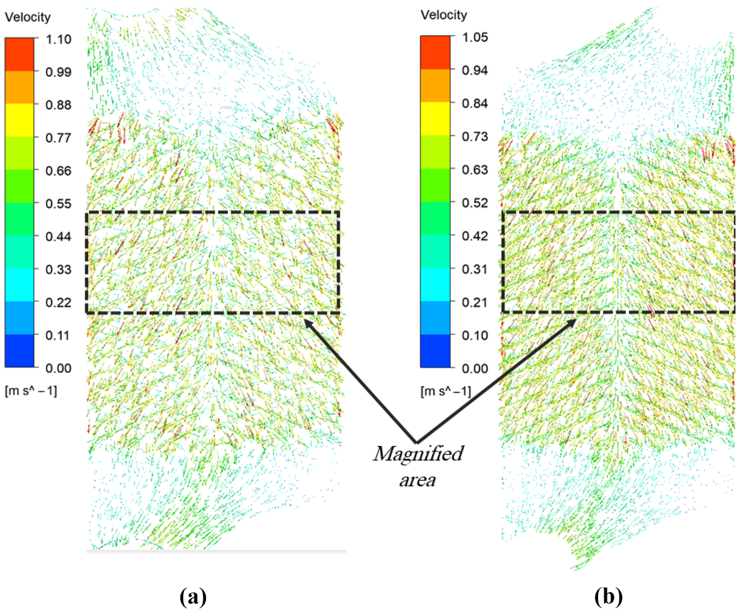

Source(s): Figure by author

Figure 7.
Velocity vectors inside hot channel for (a) vertical flow configuration and (b) diagonal flow configuration

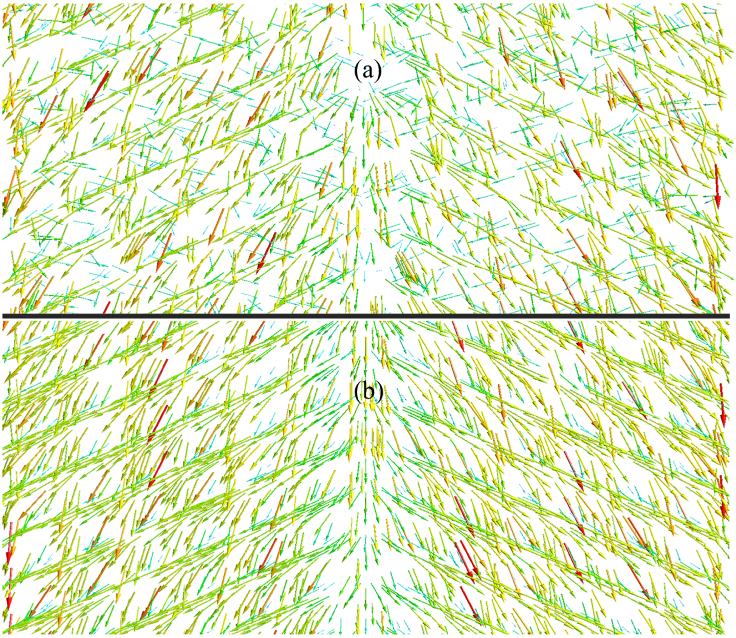

Figure 8. Magnified velocity vectors inside hot channel of (a) vertical flow configuration and (b) diagonal flow configuration

Source(s): Figure by author

Lozano *et al.* (2008), which examined the fluid flow behavior within CPHE. Moreover, the flow analysis reveals that the diagonal configuration in CPHEs exhibits both a higher magnitude and quantity of fluid flow, as evidenced in Figure 8b, in comparison to the vertical configuration illustrated in Figure 8a. Although this observation suggests that CPHEs with a diagonal configuration may exhibit enhanced flow distribution, additional investigations are required to comprehensively compare the uniformity of flow within each configuration.

5.2 Effect of flow arrangement on heat transfer

The primary purpose of any HE is to maximize heat transfer between fluids at different temperatures while maintaining physical separation between them. This objective is essential for conserving energy, improving system performance and minimizing resource consumption. Since the differences in heat transfer amounts ($\dot{Q}$) between $CPHE_{vert.}$ and $CPHE_{diag.}$ are found minimal, they are exhibited in Table 2 for sake of clarity.

Table 2. Comparison of $\dot{Q}$ variation of $CPHE_{vert.}$ and $CPHE_{diag.}$ with Re

Re	Heat transfer rate (Watt) $CPHE_{vert.}$	Heat transfer rate (Watt) $CPHE_{diag.}$
500	184.4	185.38
1,000	285.3	287.28
1,500	364.335	369.78
2,000	433.423	437.06
2,500	495.44	509.50
3,000	551.43	567.20

Source(s): Table by author

Table 2 reveals that $\dot{Q}$ values for $CPHE_{diag.}$ are generally higher than those for $CPHE_{vert.}$, showing an increase ranging from 0.5 to 2.9%. This difference can be explained by the unique flow pattern in $CPHE_{diag.}$ Here, the fluid is directed towards the opposite side of the inlet before leaving the HE. As a result, the fluid travels a longer path between the plates compared to the vertical flow configuration. The increased flow path allows for more extended contact time between the fluid and the heat transfer surfaces, facilitating greater heat transfer. The longer path also provides more surface area for heat exchange, contributing to enhanced heat transfer performance.

Figure 9a and b represents the temperature profile along the outlet axis at Re = 500 and Re = 3,000 for vertical and diagonal flow arrangements. In both flow arrangements, the temperature at the beginning is high and gradually decreases as the fluid moves along the x axis as exhibited in Figure 5 (outlet axis). This initial high temperature is due to the fact that

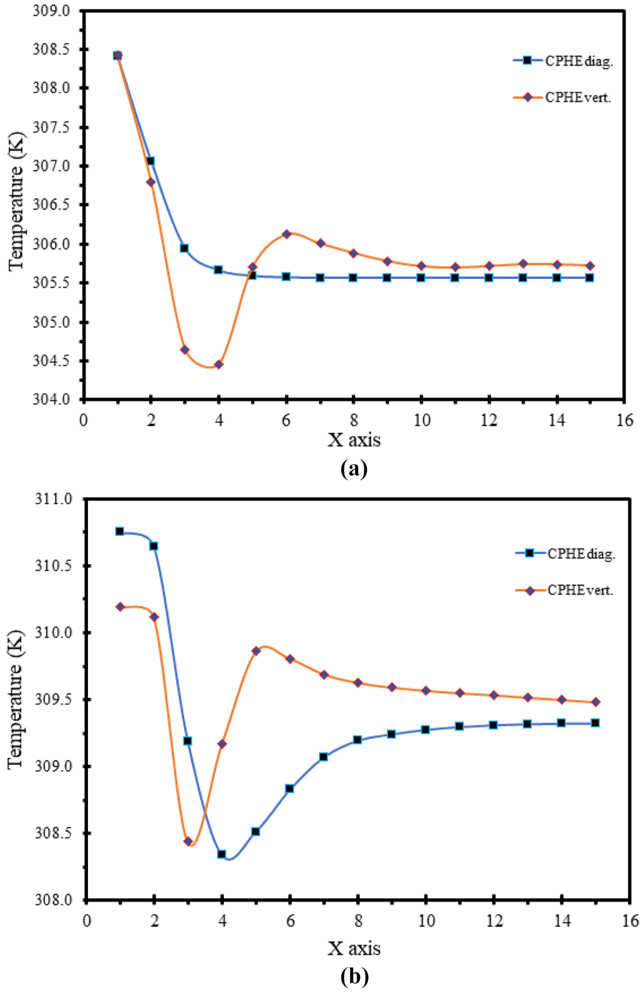

Source(s): Figure by author

Figure 9. Temperature variation along the hot channel's outlet axis for diagonal and vertical flow arrangements at, (a) Re = 500, and (b) Re = 3,000

the last channel is only in contact to a single cold channel (end channel). As the fluid progresses and mixes with the hot fluid from the first channel, which is surrounded by two cold channels, the temperature decreases further. Eventually, the temperature stabilizes and becomes relatively constant as the fluid reaches the end of the outlet axis. Moreover, Figure 9b shows the temperature profile at Re = 3,000 for vertical and diagonal flow arrangements. Similar to Figure 9a, the temperature decreases along the outlet axis. However, at Re = 3,000 the initial temperature and the bulk temperature at the end of the channel are higher with respect to that at Re = 500. This observation can be attributed to the reduced influence of viscous forces in dissipating heat at higher Re, while inertial forces become more dominant. In addition, the bulk temperature in case of diagonal flow is found lower than that in case of vertical flow at both Reynolds numbers.

Overall, both figures highlight the effect of the flow arrangement on the outlet temperature of the hot channel. The diagonal flow arrangement is found to promote more flow mixing, leading to a greater temperature drop compared to the vertical flow arrangement. The diagonal arrangement is advantageous in terms of maximizing heat transfer between the fluids, as it enhances temperature decreasing rate.

5.3 Effect of flow arrangement on pressure drop

The importance of pressure drop in the context of HEs lies in its direct impact on system efficiency and performance. The reduction in fluid pressure as it traverses a HE, is a critical parameter that warrants careful consideration in the design and operation of these thermal devices. Striking a balance between maximizing heat transfer rates and minimizing pressure drop is essential for optimizing overall system efficiency. Excessive pressure drop can lead to increased energy consumption, higher pumping requirements, and elevated operational costs. Therefore, engineers focus on designing HEs with configurations that enhance heat transfer efficiency while keeping pressure drop within acceptable limits. This delicate equilibrium is crucial across various applications, irrespective of industry, as it ensures that HEs operate efficiently without compromising on the energy conservation goals of a given system. In essence, recognizing and managing the importance of pressure drop is fundamental to achieving the desired effectiveness and sustainability of heat exchange processes.

Owing to the marginal variations in pressure drop data between $CPHE_{vert.}$ and $CPHE_{diag.}$, they are also presented in Table 3 for sake of clarity. A comprehensive scrutiny of Table 3 unveils a consistent pattern wherein the pressure drop values for $CPHE_{vert.}$ consistently exceed those for $CPHE_{diag.}$ across the entire Re range. Specifically, the observed differences range from 3% to 9.23%, with the most notable divergence occurring at Re = 1,500.

The reason of higher ΔP in case of vertical flow configuration could be owing to the higher flow velocity compared to the diagonal flow configuration as shown earlier in Figure 6. The increased velocity leads to greater frictional losses and pressure drop. Also, the vertical flow configuration tends to have a higher head loss due to the pressure drop associated with changes in fluid elevation. As the fluid moves vertically, it encounters changes in height, resulting in

Table 3. Comparison of pressure drop variation of $CPHE_{vert.}$ and $CPHE_{diag.}$ with Re

Re	Pressure drop (kW) $CPHE_{vert.}$	Pressure drop (kW) $CPHE_{diag.}$
500	6.17	5.81
1,000	21.58	20.63
1,500	45.91	41.678
2,000	79.52	77.15
2,500	122.58	115.58
3,000	175.10	168.34

Source(s): Table by author

additional pressure losses. In the diagonal flow configuration, the fluid moves diagonally across the plates, minimizing the elevation changes and reducing the pressure drop.

6. Dimensionless performance metrics

Although the dimensions of the present CPHEs are identical, dimensionless metrics are presented to express quantities in a standardized form, allowing for meaningful comparisons and generalizations. A comparison between data of Nusselt number (Nu) of $CPHE_{vert.}$ and $CPHE_{diag.}$ is displayed in Table 4. Notably, the Nu data pertaining to $CPHE_{diag.}$ consistently exhibit higher values compared to $CPHE_{vert.}$ across the entire range of Re. Nevertheless, these differences are marginal and similar to the trends observed in the earlier analysis of $\dot{Q}$ data.

Fanning friction factor (*f*) is a parameter used to quantify the resistance encountered by the fluid during its flow within the present CPHEs. Figure 10 displays the results of the *f* data for both the vertical and diagonal flow arrangements. It is evident from Figure 10 that the *f* values associated with $CPHE_{vert.}$ are consistently higher than those of $CPHE_{diag.}$ across the entire range of Re. This difference in *f* values can be attributed to the characteristics of the fluid flow within the CPHE arrangements. As mentioned previously, the fluid inside $CPHE_{diag.}$ exhibits a more favorable flow distribution and flows at a lower velocity compared to $CPHE_{vert.}$. These factors contribute to reduced resistance and subsequently lower *f* values for $CPHE_{diag.}$.

The JF factor is a dimensionless parameter widely employed as a comprehensive metric for assessing the overall thermal performance, and it is utilized to compare the performance of the present CPHEs. The Colburn factor (j) is another dimensionless parameter that provides a comprehensive assessment of convective heat transfer efficiency, accounting for both fluid flow and thermal properties.

$$j = \frac{Nu}{RePr^{1/3}} \tag{14}$$

$$JF = \frac{(j/j_o)}{(f/f_o)^{1/3}} \tag{15}$$

Where Pr stands for Prandtl number, j_o and f_o represent j and f of the flat plate heat exchanger (FPHE), respectively. Table 5 presents the JF factor results for $CPHE_{vert.}$ and $CPHE_{diag.}$ at various Re. The data in Table 5 indicate that the JF values for $CPHE_{diag.}$ consistently surpass those of $CPHE_{vert.}$ across the entire range of Re. Moreover, from the aforementioned discussion Nu data of $CPHE_{diag.}$ are found to be larger and the concurrent *f* data are lower with respect to those of the $CPHE_{vert.}$. Therefore, the data on the JF factor are found to be greater in the case of $CPHE_{diag.}$ as expected.

Re	Nu $CPHE_{vert.}$	Nu $CPHE_{diag.}$
500	20.6	20.71
1,000	31.6	31.82
1,500	40.65	41.26
2,000	49.5	49.92
2,500	58.31	59.96
3,000	66.15	68.04

Source(s): Table by author

Table 4. Comparison of Nu data variation of $CPHE_{vert.}$ and $CPHE_{diag.}$ with Re

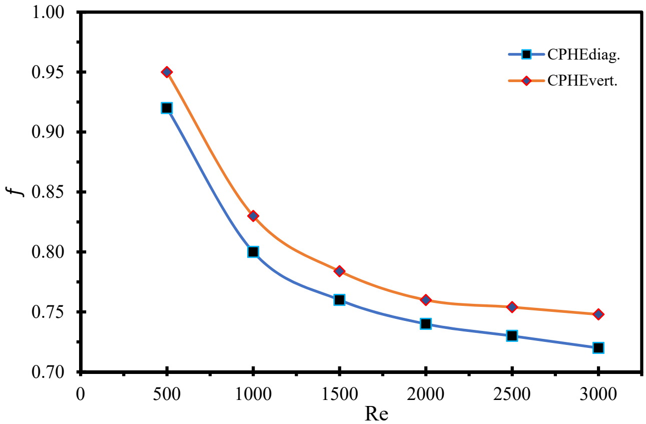

Source(s): Figure by author

Figure 10. Comparison between f results of the diagonal and vertical flow arrangements

Table 5. Comparison of JF factor results of $CPHE_{vert.}$ and $CPHE_{diag.}$

Re	JF ($CPHE_{vert.}$)	JF ($CPHE_{diag.}$)
500	1.10	1.13
1,000	0.94	0.95
1,500	0.95	0.98
2,000	0.93	0.95
2,500	0.93	0.97
3,000	0.84	0.88

Source(s): Table by author

The ratio of heat transfer to the required pumping power (η) is a dimensionless parameter, and it is employed in the present study to compare the power consumption associated with the present CPHEs.

$$PP = \dot{m}\Delta P_t/\rho \tag{16}$$

$$\eta = \dot{Q}/PP \tag{17}$$

The variations in η for the vertical and diagonal flow arrangements with Re are presented in Table 6. It indicates that η of $CPHE_{diag.}$ are 4–11.8% greater than those of the $CPHE_{vert.}$. This shows that $CPHE_{diag.}$ exhibits higher energy efficiency, achieving a greater amount of heat transfer per unit of pumping power compared to $CPHE_{vert.}$. Similarly, as discussed earlier, the heat transfer rate ($\dot{Q}$) for $CPHE_{diag.}$ is found to be larger, while the corresponding pressure

Table 6. Comparison of η variation of $CPHE_{vert.}$ and $CPHE_{diag.}$ with Re

Re	η ($CPHE_{vert.}$)	η ($CPHE_{diag.}$)
500	5,043.31	5,386.42
1,000	1,116.08	1,175.51
1,500	446.61	499.35
2,000	230.05	239.13
2,500	136.48	148.86
3,000	88.62	94.81

Source(s): Table by author

drops are lower compared to $CPHE_{vert.}$. These findings reinforce the superior performance of $CPHE_{diag.}$ in terms of heat transfer efficiency and reduced energy consumption.

Overall, the present study thoroughly investigated the impact of vertical and diagonal flow arrangements on the thermal performance of the CPHE. The diagonal flow arrangement is found to promote greater flow mixing and resulted in a higher temperature drop along the outlet axis compared to the vertical flow arrangement. Also, the diagonal flow arrangement is found to yield greater JF and η values compared to the vertical flow arrangement. Thereby, the diagonal flow arrangement demonstrates advantages in terms of heat transfer and pumping power, indicating its potential in comparison with the vertical one.

7. Conclusions

The present study examined the thermal performance of two CPHEs featuring different flow arrangements: one with a vertical flow configuration and the other with a diagonal flow configuration. Both HEs have identical geometrical dimensions and operating conditions. The key conclusions of this investigation are as follows:

(1) Both $CPHE_{vert.}$ and $CPHE_{diag.}$ exhibited similar flow behavior, with high and low velocity vectors distributed sideways away from the middle of the channel. However, the diagonal flow configuration showed a higher magnitude and quantity of fluid flow.

(2) The difference in data of heat transfer amount ($\dot{Q}$) between $CPHE_{vert.}$ and $CPHE_{diag.}$ showed minimal differences. However, $CPHE_{diag.}$ consistently exhibited higher heat transfer rates ranging from 0.5 to 2.9%, attributed to the longer flow path and increased contact time between the fluid and heat transfer surfaces. Similarly, Nu data pertaining to $CPHE_{diag.}$ consistently exhibit higher values compared to $CPHE_{vert.}$. across the entire range of Re.

(3) $CPHE_{vert.}$ consistently revealed higher pressure drop values compared to $CPHE_{diag.}$ across the entire Re range. Likewise, f values associated with $CPHE_{vert.}$. were consistently found to be higher than those of $CPHE_{diag.}$ across the entire range of Re.

(4) The overall thermal performance of $CPHE_{diag.}$ and $CPHE_{vert.}$. has been estimated by calculating JF and the ratio of heat transfer to the pumping power (η). Both JF and η of $CPHE_{diag.}$ are found to be greater than those of $CPHE_{vert.}$.

Overall, these results indicate that the diagonal flow configuration in CPHEs offers improved flow distribution, enhanced heat transfer performance and a lower pressure drop compared to the vertical flow configuration. However, the differences in general in the thermal performance of $CPHE_{vert.}$and $CPHE_{diag.}$ are found to be minimal. Future studies are encouraged to investigate the impact of fouling on the thermal performance of CPHEs with vertical and diagonal flow arrangements. Additionally, conducting an economic feasibility comparison will help determine the most efficient and cost-effective option for industrial applications.

References

Al-Zahrani, S., Islam, M.S. and Saha, S.C. (2019), "A thermo-hydraulic characteristics investigation in corrugated plate heat exchanger", *Energy Procedia*, Vol. 160, pp. 597-605, doi: 10.1016/j.egypro.2019.02.211.

Al-Zahrani, S., Islam, M.S. and Saha, S.C. (2020a), "Heat transfer augmentation in retrofitted corrugated plate heat exchanger", *International Journal of Heat and Mass Transfer*, Vol. 161, 120226, doi: 10.1016/j.ijheatmasstransfer.2020.120226.

Al-Zahrani, S., Islam, M.S., Xu, F. and Saha, S.C. (2020b), "Thermal performance investigation in a novel corrugated plate heat exchanger", *International Journal of Heat and Mass Transfer*, Vol. 148, 119095, doi: 10.1016/j.ijheatmasstransfer.2019.119095.

Al-Zahrani, S., Islam, M.S. and Saha, S.C. (2021a), "Heat transfer enhancement investigation in a novel flat plate heat exchanger", *International Journal of Thermal Sciences*, Vol. 161, 106763, doi: 10.1016/j.ijthermalsci.2020.106763.

Al-Zahrani, S., Islam, M.S. and Saha, S.C. (2021b), "Comparison of flow resistance and port maldistribution between novel and conventional plate heat exchangers", *International Communications in Heat and Mass Transfer*, Vol. 123, 105200, doi: 10.1016/j.icheatmasstransfer.2021.105200.

Al-Zahrani, S., Islam, M.S. and Saha, S.C. (2021c), "Heat transfer enhancement of modified flat plate heat exchanger", *Applied Thermal Engineering*, Vol. 186, 116533, doi: 10.1016/j.applthermaleng.2020.116533.

Alfwzan, W.F., Alomani, G.A., Alessa, L.A. and Selim, M.M. (2023), "Nanofluid heat transfer and flow characteristics in a convex plate heat exchanger based on multi-objective optimization", *Journal of Nanoelectronics and Optoelectronics*, Vol. 18 No. 10, pp. 1239-1253, doi: 10.1166/jno.2023.3505.

ANSYS (2009), *ANSYS Fluent 12.0 User's Guide*, ANSYS, PA.

ANSYS (n.d.), *ANSYS Fluent User's Guide*, available at: http://www.pmt.usp.br/academic/martoran/notasmodelosgrad/ANSYS%20Fluent%20Users%20Guide.pdf (accessed 7 February 2023).

Ayub, Z.H. (2003), "Plate heat exchanger literature survey and new heat transfer and pressure drop correlations for refrigerant evaporators", *Heat Transfer Engineering*, Vol. 24 No. 5, pp. 3-16, doi: 10.1080/01457630304056.

Berce, J., Zupančič, M., Može, M. and Golobič, I. (2023), "Infrared thermography observations of crystallization fouling in a plate heat exchanger", *Applied Thermal Engineering*, Vol. 224, 120116, doi: 10.1016/j.applthermaleng.2023.120116.

Borjigin, S., Zhang, S., Ma, T., Zeng, M. and Wang, Q. (2020), "Performance enhancement of cabinet cooling system by utilizing cross-flow plate heat exchanger", *Energy Conversion and Management*, Vol. 213, 112854, doi: 10.1016/j.enconman.2020.112854.

Chen, W.-H., Li, Y.W., Chang, M.H., Chueh, C.C., Ashokkumar, V. and Saw, L.H. (2022), "Operation and multi-objective design optimization of a plate heat exchanger with zigzag Flow Channel geometry", *Energies*, Vol. 15 No. 21, p. 8205, doi: 10.3390/en15218205.

Cooper, A. and Usher, J.D. (1983), "Heat exchanger design handbook", in *Method Surf. Area Calc*, VDI-Verlag, Hemisphere Publishing.

Durmuş, A., Benli, H., Kurtbaş, İ. and Gül, H. (2009), "Investigation of heat transfer and pressure drop in plate heat exchangers having different surface profiles", *International Journal of Heat and Mass Transfer*, Vol. 52 Nos 5-6, pp. 1451-1457, doi: 10.1016/j.ijheatmasstransfer.2008.07.052.

Elias, M., Rahman, S., Rahim, N., Sohel, M. and Mahbubul, I. (2014), "Performance investigation of a plate heat exchanger using nanofluid with different chevron angle", *Advanced Materials Research*, Vol. 832, pp. 254-259, doi: 10.4028/www.scientific.net/amr.832.254.

Gherasim, I., Galanis, N. and Nguyen, C.T. (2011), "Heat transfer and fluid flow in a plate heat exchanger. Part II: assessment of laminar and two-equation turbulent models", *International Journal of Thermal Sciences*, Vol. 50 No. 8, pp. 1499-1511, doi: 10.1016/j.ijthermalsci.2011.03.017.

Göltaş, M., Gürel, B., Keçebaş, A., Akkaya, V.R. and Güler, O.V. (2022), "Improvement of thermo-hydraulic performance with plate surface geometry for a compact plate heat exchanger manufactured by additive manufacturing", *International Journal of Heat and Mass Transfer*, Vol. 188, 122637, doi: 10.1016/j.ijheatmasstransfer.2022.122637.

Ham, J., Yong, J., Kwon, O., Bae, K. and Cho, H. (2023), "Experimental investigation on heat transfer and pressure drop of brazed plate heat exchanger using LiBr solution", *Applied Thermal Engineering*, Vol. 225, 120161, doi: 10.1016/j.applthermaleng.2023.120161.

Islamoglu, Y. and Parmaksizoglu, C. (2003), "The effect of channel height on the enhanced heat transfer characteristics in a corrugated heat exchanger channel", *Applied Thermal Engineering*, Vol. 23 No. 8, pp. 979-987, doi: 10.1016/s1359-4311(03)00029-2.

Jin, Y., Li, M., Cui, J. and Li, Z. (2024), "Study on the thermal performance of the cross-flow plate heat exchangers", *Numerical Heat Transfer, Part A: Applications*, Vol. 23, pp. 1-21, doi: 10.1080/10407782.2024.2310594.

Kan, M., Ipek, O. and Gurel, B. (2015), "Plate heat exchangers as a compact design and optimization of different channel angles", *Acta Physica Polonica A*, Vol. 128 No. 2B, pp. B-49-B-52, doi: 10.12693/aphyspola.128.b-49.

Khan, T., Khan, M., Chyu, M.C. and Ayub, Z. (2010), "Experimental investigation of single phase convective heat transfer coefficient in a corrugated plate heat exchanger for multiple plate configurations", *Applied Thermal Engineering*, Vol. 30 Nos 8-9, pp. 1058-1065, doi: 10.1016/j.applthermaleng.2010.01.021.

Kılıç, B. and İpek, O. (2017), "Experimental investigation of heat transfer and effectiveness in corrugated plate heat exchangers having different chevron angles", *Heat and Mass Transfer*, Vol. 53 No. 2, pp. 725-731, doi: 10.1007/s00231-016-1817-2.

Kumar, B., Soni, A. and Singh, S. (2018), "Effect of geometrical parameters on the performance of chevron type plate heat exchanger", *Experimental Thermal and Fluid Science*, Vol. 91, pp. 126-133, doi: 10.1016/j.expthermflusci.2017.09.023.

Kwon, O.-k., Cha, D.A., Yun, J.H. and Kim, H.S. (2009), "Performance evaluation of plate heat exchanger with chevron angle variations", *Transactions of the Korean Society of Mechanical Engineers B*, Vol. 33 No. 7, pp. 520-526, doi: 10.3795/ksme-b.2009.33.7.520.

Lee, J. and Lee, K.-S. (2013), "Correlations and shape optimization in a channel with aligned dimples and protrusions", *International Journal of Heat and Mass Transfer*, Vol. 64, pp. 444-451, doi: 10.1016/j.ijheatmasstransfer.2013.04.055.

Lee, J. and Lee, K.-S. (2014), "Flow characteristics and thermal performance in chevron type plate heat exchangers", *International Journal of Heat and Mass Transfer*, Vol. 78, pp. 699-706, doi: 10.1016/j.ijheatmasstransfer.2014.07.033.

Lee, J. and Lee, K.-S. (2015), "Friction and Colburn factor correlations and shape optimization of chevron-type plate heat exchangers", *Applied Thermal Engineering*, Vol. 89, pp. 62-69, doi: 10.1016/j.applthermaleng.2015.05.080.

Li, Q., Flamant, G., Yuan, X., Neveu, P. and Luo, L. (2011), "Compact heat exchangers: a review and future applications for a new generation of high temperature solar receivers", *Renewable and Sustainable Energy Reviews*, Vol. 15 No. 9, pp. 4855-4875, doi: 10.1016/j.rser.2011.07.066.

Lozano, A., Barreras, F., Fueyo, N. and Santodomingo, S. (2008), "The flow in an oil/water plate heat exchanger for the automotive industry", *Applied Thermal Engineering*, Vol. 28 No. 10, pp. 1109-1117, doi: 10.1016/j.applthermaleng.2007.08.015.

Marouf, Z.M., Fouad, M.A. and Hassan, M.A. (2022), "Experimental investigation of the effect of air bubbles injection on the performance of a plate heat exchanger", *Applied Thermal Engineering*, Vol. 217, 119264, doi: 10.1016/j.applthermaleng.2022.119264.

Meng, L., Liu, J., Bi, J., Özdemir, E.D. and Aksel, M.H. (2023), "Multi-objective optimization of plate heat exchanger for commercial electric vehicle based on genetic algorithm", *Case Studies in Thermal Engineering*, Vol. 41, 102629, doi: 10.1016/j.csite.2022.102629.

Mikhaeil, M., Nowak, S., Palomba, V., Frazzica, A., Gaderer, M. and Dawoud, B. (2023), "Experimental and analytical investigation of applying an asymmetric plate heat exchanger as an evaporator in a thermally driven adsorption appliance", *Applied Thermal Engineering*, Vol. 228, 120525, doi: 10.1016/j.applthermaleng.2023.120525.

Nguyen, D.H., Kweon, B., Kwon, J.S., Kim, T., Wongwises, S. and Ahn, H.S. (2022), "Numerical study on novel airfoil corrugated plate heat exchanger: a comparison with commercial type and geometrical parameter analysis", *International Journal of Heat and Mass Transfer*, Vol. 195, 123119, doi: 10.1016/j.ijheatmasstransfer.2022.123119.

Nguyen, D.H., Quoc Nguyen, P., Ur Rehman, R., Kim, J.F. and Seon Ahn, H. (2024), "Optimizing the effect of micro-surface on the thermal hydraulic performance of plate heat exchanger", *Applied Thermal Engineering*, Vol. 239, 122172, doi: 10.1016/j.applthermaleng.2023.122172.

Panday, N.K. and Singh, S.N. (2022), "Study of thermo-hydraulic performance of chevron type plate heat exchanger with wire inserts in the channel", *International Journal of Thermal Sciences*, Vol. 173, 107360, doi: 10.1016/j.ijthermalsci.2021.107360.

Saha, S.K. and Khan, A.H. (2020), "Numerical study on the effect of corrugation angle on thermal performance of cross corrugated plate heat exchangers", *Thermal Science and Engineering Progress*, Vol. 20, 100711, doi: 10.1016/j.tsep.2020.100711.

Shokouhmand, H. and Hasanpour, M. (2020), "Effect of flow maldistribution on the optimal design of plate heat exchanger using constrained multi objective genetic algorithm", *Case Studies in Thermal Engineering*, Vol. 18, 100570, doi: 10.1016/j.csite.2019.100570.

Sundén, B. and Manglik, R.M. (2007), *Plate Heat Exchangers: Design, Applications and Performance*, Wit Press, Ashurst Lodge, Vol. 11.

Syed, A. (1992), "The use of plate heat exchangers as evaporators and condensers in process refrigeration", *Heat Exchange Engineering*.

Tavallaei, M., Farzaneh-Gord, M., Moghadam, A.J. and Ebrahimi-Moghadam, A. (2023), "Parametric study and optimization of pillow-plate heat exchanger using multi-objective genetic algorithm and entropy generation minimization approaches", *Heat and Mass Transfer*, Vol. 59 No. 9, pp. 1687-1706, doi: 10.1007/s00231-023-03363-x.

Vitillo, F., Cachon, L., Reulet, P., Laroche, E. and Millan, P. (2015), "An innovative plate heat exchanger of enhanced compactness", *Applied Thermal Engineering*, Vol. 87, pp. 826-838, doi: 10.1016/j.applthermaleng.2015.05.019.

Wang, D., Zhang, H., Wang, G., Yuan, H. and Peng, X. (2023), "Experimental and numerical study on the heat transfer and flow characteristics of convex plate heat exchanger based on multi-objective optimization", *International Journal of Heat and Mass Transfer*, Vol. 202, 123755, doi: 10.1016/j.ijheatmasstransfer.2022.123755.

World Energy Outlook (n.d.), "2014 world energy Outlook, executive summary", available at: https://eneken.ieej.or.jp/data/5794.pdf (accessed 8.November.2020).

Yicong, L., Chunyu, S., Wei, L. and Zhichun, L. (2023), "Structural parameter design of welded plate heat exchanger based on multi-objective optimization algorithm", *International Communications in Heat and Mass Transfer*, Vol. 146, 106900, doi: 10.1016/j.icheatmasstransfer.2023.106900.

Yu, C., Shao, M., Zhang, W., Wang, G. and Huang, M. (2024), "Study on heat transfer synergy and optimization of capsule-type plate heat exchangers", *Processes*, Vol. 12 No. 3, p. 604, doi: 10.3390/pr12030604.

Zhang, J., Zhu, X., Mondejar, M.E. and Haglind, F. (2019), "A review of heat transfer enhancement techniques in plate heat exchangers", *Renewable and Sustainable Energy Reviews*, Vol. 101, pp. 305-328, doi: 10.1016/j.rser.2018.11.017.

Zhu, X. and Haglind, F. (2020), "Relationship between inclination angle and friction factor of chevron-type plate heat exchangers", *International Journal of Heat and Mass Transfer*, Vol. 162, 120370, doi: 10.1016/j.ijheatmasstransfer.2020.120370.

Corresponding author
Salman Al-Zahrani can be contacted at: salman.zahrani@bu.edu.sa